

# THE SPATIALLY RESOLVED STAR FORMATION LAW FROM INTEGRAL FIELD SPECTROSCOPY

Guillermo A. Blanc, Amanda Heiderman, Karl Gebhardt, and Neal J. Evans II  
The University of Texas at Austin



## INTRODUCTION

We study the “spatially resolved” Star Formation Law (SFL), that is, the relation between the SFR surface density ( $\Sigma_{\text{SFR}}$ ) and the atomic, molecular, and total gas surface densities ( $\Sigma_{\text{HI}}$ ,  $\Sigma_{\text{H}_2}$ , and  $\Sigma_{\text{HI}+\text{H}_2}$ ) in  $\sim 200$  pc scales throughout the disk of the nearby face-on Sbc galaxy NGC 5194 (a.k.a. M51a, The Whirlpool Galaxy).

Recent studies of the spatially resolved SFL disagree in the behavior of the molecular component. Kennicutt et al. (2007) measures a super-linear slope  $N = 1.37 \pm 0.03$  for the molecular gas SFL in NGC 5194, which suggests an increasing star formation efficiency ( $\text{SFE} = \Sigma_{\text{SFR}} / \Sigma_{\text{H}_2}$ ) towards higher gas densities. Bigiel et al (2008) on the other hand, measures a molecular SFL with an average  $N = 1.0 \pm 0.2$  for a sample of 7 normal spirals ( $N = 0.84$  for NGC 5194), consistent with a scenario in which star formation occurs at a constant efficiency inside GMCs, whose properties are fairly uniform across normal spiral galaxies (Blitz et al. 2007, Bolatto et al. 2008).

With the goal of investigating this issue, we conduct the first measurement of the spatially resolved SFL using integral field spectroscopy. Using data from the VIRUS-P Exploration of Nearby Galaxies (VENGA), we measure H $\alpha$ , H $\beta$ , [NII] $\lambda\lambda 6548, 6584$ , and [SII] $\lambda\lambda 6717, 6731$  emission line fluxes of 735 regions  $\sim 170$  pc in diameter over the central  $4.1 \times 4.1$  kpc<sup>2</sup> of the galaxy. These lines are used to estimate dust extinctions, separate the contribution to the H $\alpha$  flux from HII regions in the disk and the diffuse ionized gas (DIG), and measure accurate SFRs. Atomic and molecular gas surface densities are measured using the THINGS 21cm (Walter et al. 2008) and BIMA SONG CO J=1-0 (Helfer et al. 2003) intensity maps of NCG 5194.

Integral field spectroscopy allows a much cleaner measurement of the H $\alpha$  emission than narrow-band imaging, since it is free of the systematics introduced by continuum subtraction, underlying photospheric absorption, and contamination by the [NII] doublet.

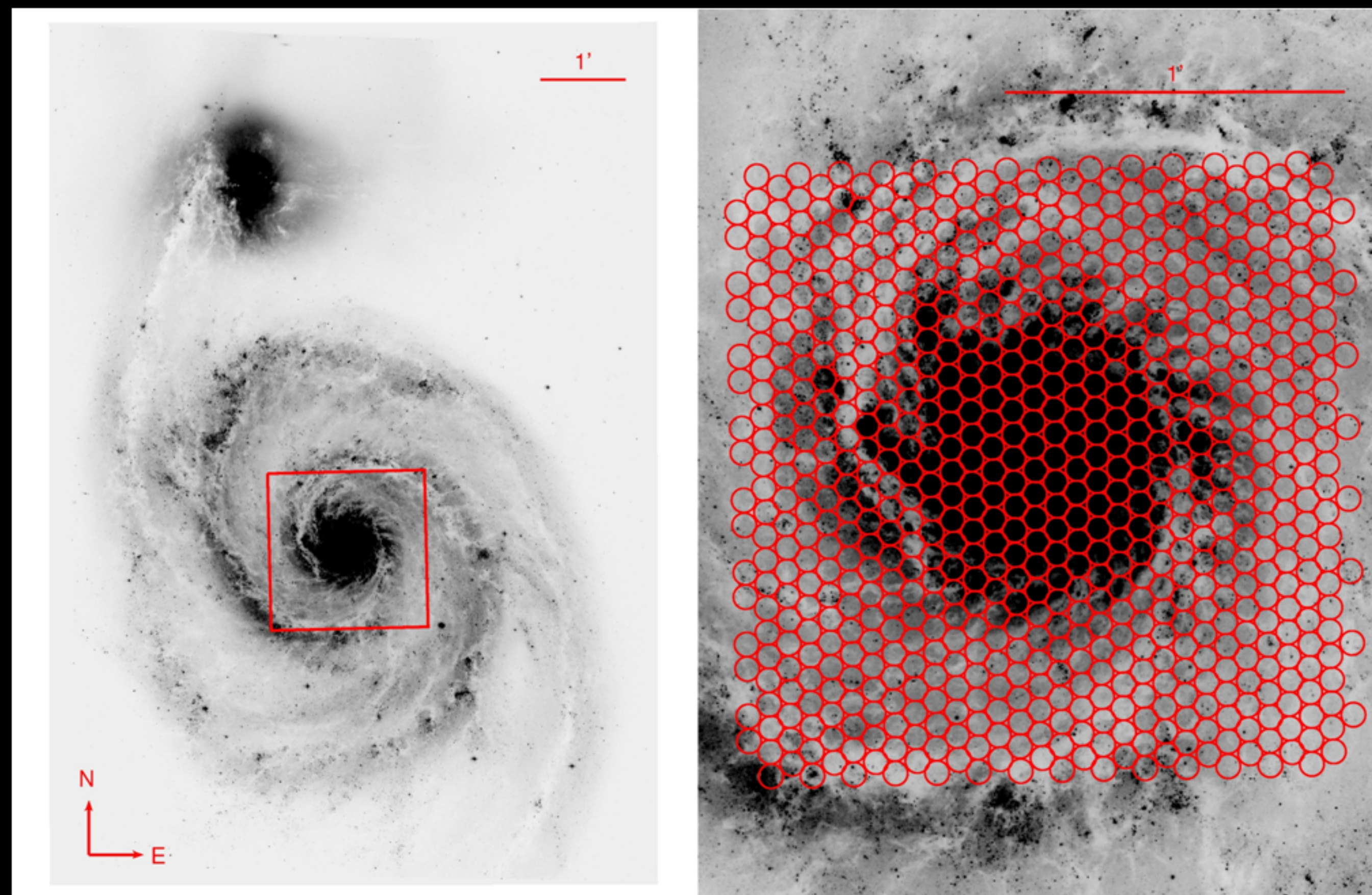


Figure 1: HST V-band image of NGC 5194. The VIRUS-P field of view is shown as the red square in the left panel. VIRUS-P is a large field of view fiber-fed integral field spectrograph. The regions sampled by the fibers during the observations are shown as red circles in the right panel.

## EXTINCTION CORRECTION

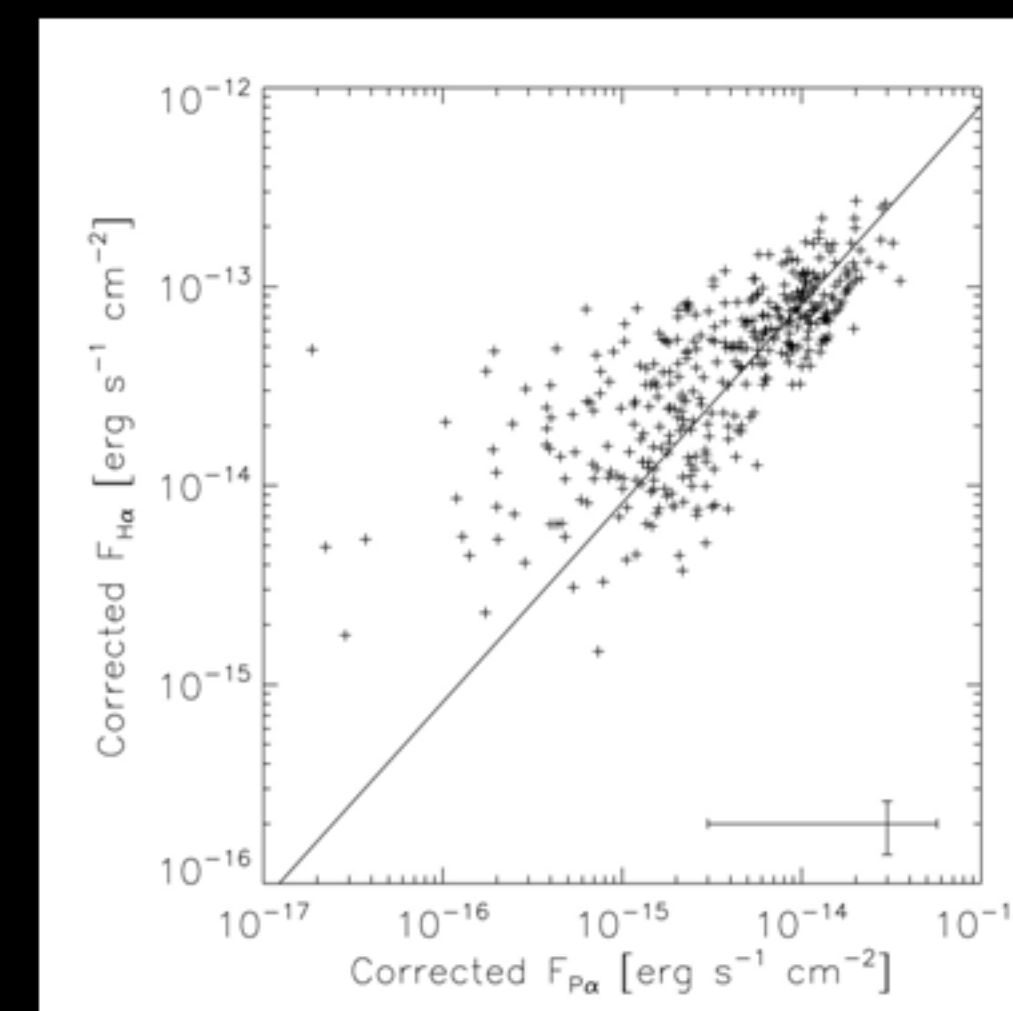


Figure 3: We use the Balmer decrement to estimate the nebular dust extinction for each region and correct the H $\alpha$  flux before estimating the SFR. The figure shows the extinction corrected Paa flux (measured in the NICMOS narrow-band image of Scoville et al. 2001) versus the extinction corrected VIRUS-P H $\alpha$  flux for all regions detected in Paa. The solid line marks the theoretical intrinsic line ratio of 8.15 predicted by recombination theory which is in good agreement with the data. This confirms that H $\alpha$  fluxes, once corrected for dust obscuration using the Balmer decrement, can provide an unbiased estimate of the intrinsic SFR in the disks of normal face-on spirals.

## DIFFUSE IONIZED GAS

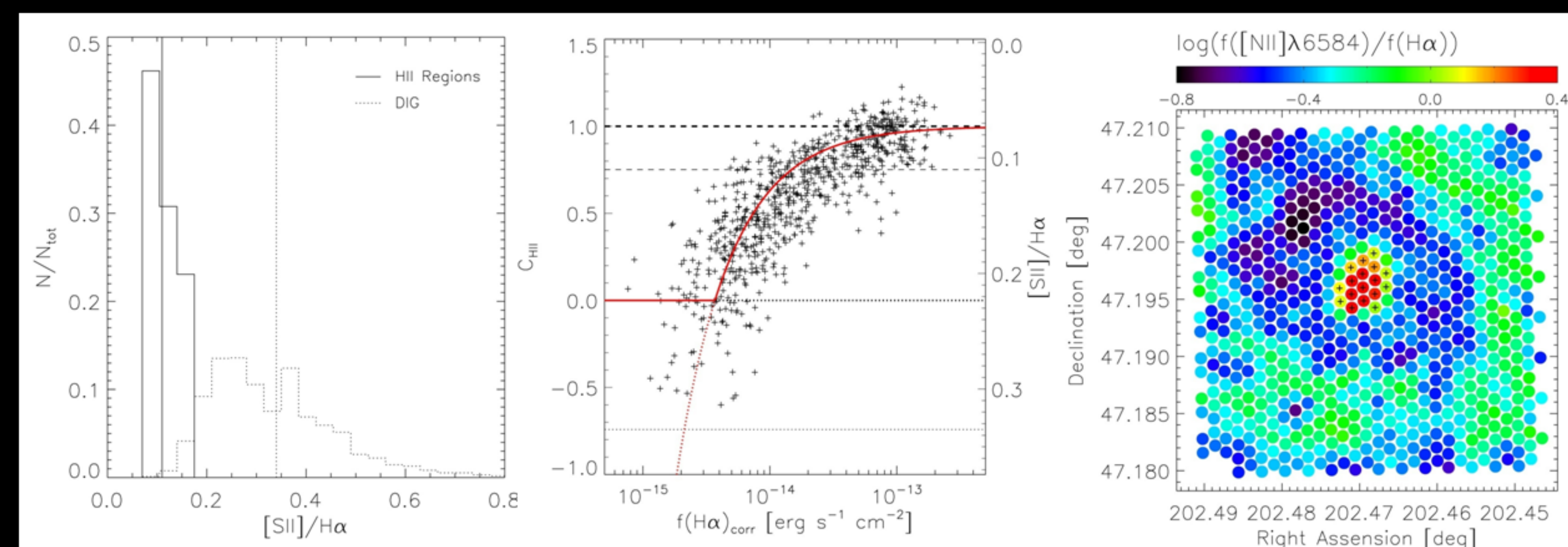


Figure 4: At any given line of sight towards the galaxy, the DIG contributes H $\alpha$  emission which is not associated with localized star formation at that same position in the disk. Low-ionization line ratios like [NII] $\lambda 6584$ /H $\alpha$  and [SII] $\lambda 6717$ /H $\alpha$  are observed to be greatly enhanced in the DIG, as compared to H II regions (Madsen et al. 2006, left panel). Hence, the large spectral coverage of the VENGA data allows us to use these line ratios to separate and subtract the DIG contribution to the H $\alpha$  fluxes. The central panel of Figure 4 shows the fraction of the H $\alpha$  flux ( $C_{\text{HII}}$ ) coming from HII regions in the disk, as computed from the [SII]/H $\alpha$  ratio measured in each region.

The two panels in Figure 5 show maps of the extinction corrected H $\alpha$  emission line flux before and after the DIG correction is applied. It can be seen clearly how the H $\alpha$  emission traces the spiral pattern of star-formation. The correction leaves the H $\alpha$  flux coming from the brightest star forming regions practically unchanged, while removing the contribution from the DIG which dominates the observed spectrum in the inter-arm regions of the galaxy. The latter can also be appreciated in the right panel of Figure 4, which shows an enhanced [NII]/H $\alpha$  ratio typical of the DIG in the inter-arm regions, and normal H II region ratios throughout the spiral arms.

**ACKNOWLEDGMENTS:**  
We acknowledge the staff at McDonald Observatory for their invaluable help during the observations. Tables of the WHAM DIG line ratios were kindly provided by George J. Madsen. We thank Daniela Calzetti for some very useful discussions, and for providing the narrow-band Paa and H $\alpha$  images used in her work. This study has been possible thanks to the financial support of the Sigma Xi Society. The construction of VIRUS-P was possible thanks to the generous support of the Cynthia & George Mitchell Foundation. NJE and AH were supported in part by NSF Grant AST-0607193.

**REFERENCES:**  
- Bigiel, F. et al. 2008, AJ, 136, 2846  
- Blitz, L. et al. 2007, Protostars and Planets V, 81  
- Bolatto, A. D. et al. 2008, ApJ, 686, 948  
- Helfer, T. Tet al. 2003, ApJS, 145, 259  
- Kennicutt, R. C., Jr., et al. 2007, ApJ, 671, 333  
- Krumholz, M. R et al. 2009, arXiv:0904.0009  
- Leroy, A. K. et al. 2008, AJ, 136, 2782  
- Madsen, G. J et al. 2006, ApJ, 652, 401  
- Scoville, N. Z. et al. 2001, AJ, 122, 3017  
- Wong, T., & Blitz, L. 2002, ApJ, 569, 157

## VENGA

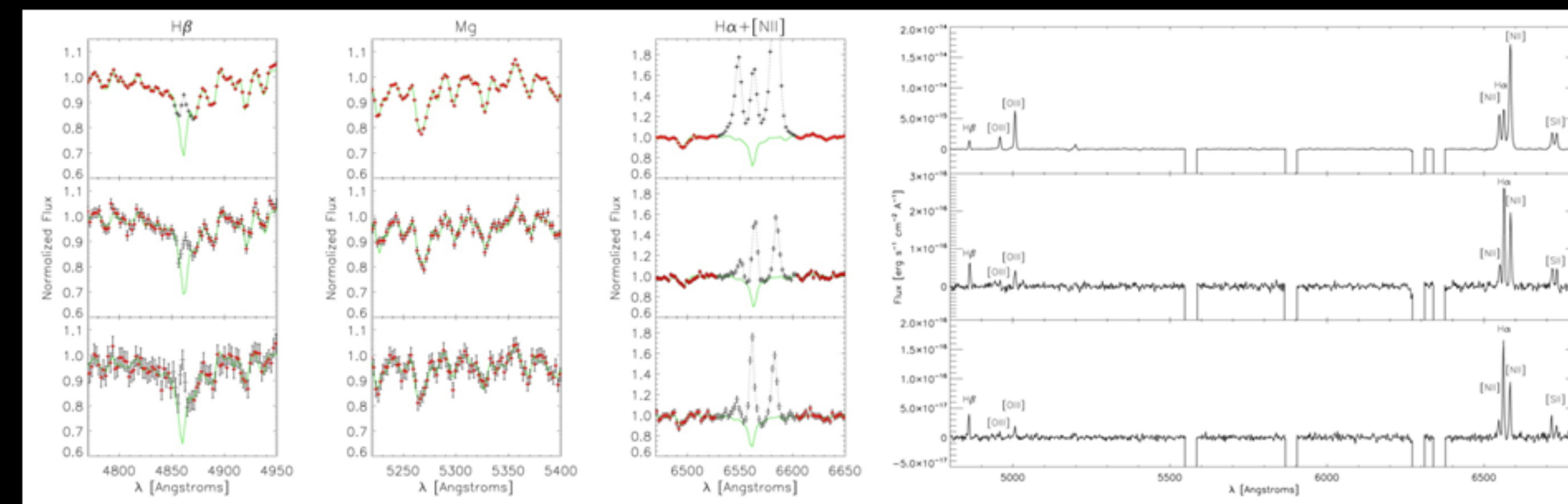


Figure 2: Spectra of the highest, median, and lowest S/N fibers on NGC 5194. The left panels are before fitting and subtracting the stellar continuum, and show how important it is to properly account for underlying Balmer absorption features when measuring emission line fluxes. The right panel shows the pure nebular spectrum. Notice how the [NII]/H $\alpha$  can change dramatically from region to region.

The VIRUS-P Exploration of Nearby Galaxies (VENGA) is an ongoing IFU survey which targets large parts of the disks of 30 nearby spiral galaxies, obtaining hundreds of spectra like the ones in Figure 2 per galaxy.

The sample spans a wide range in Hubble types, SFRs, and morphologies. Galaxies showing both classical and pseudo bulges, as well as barred and unbarred objects are present in the sample. Emphasis is given to the availability of multi-wavelength imaging. 93% of the sample has HST optical imaging, 77% has Spitzer IRAC and MIPS coverage, 60% has mid-IR IRS spectroscopy in their central parts, 97% has UV GALEX imaging, and a 63% has CO data from BIMA SONG or are part of the CARMA CO survey STINGS.

VENGA will allow a large number of researchers to conduct an extensive set of studies on star-formation, structure assembly, stellar populations, gas and stellar dynamics, chemical evolution, ISM structure, and galactic feedback, which will provide answers to many important questions in galaxy formation and evolution.

VIRUS-P is the largest field-of-view IFU in the world and allows for efficient mapping of extended low surface brightness sources like nearby galaxies.

## THE MC FITTING METHOD

We fit the molecular and total gas SFLs using a Monte Carlo (MC) approach combined with a two-dimensional distribution comparison technique. Our method allows us to include the regions not detected in the CO map (including the ones with negative measured fluxes), incorporate the intrinsic scatter in the SFL as a free parameter, and perform the fitting in linear space, avoiding the assumption of log-normal symmetric errors. For any set of parameters  $\{A, N, \epsilon\}$  we produce 200 MC realizations of the model and compare them to the data in the linear  $\Sigma_{\text{SFR}}$  vs.  $\Sigma_{\text{gas}}$  plane as shown in Figure 6.

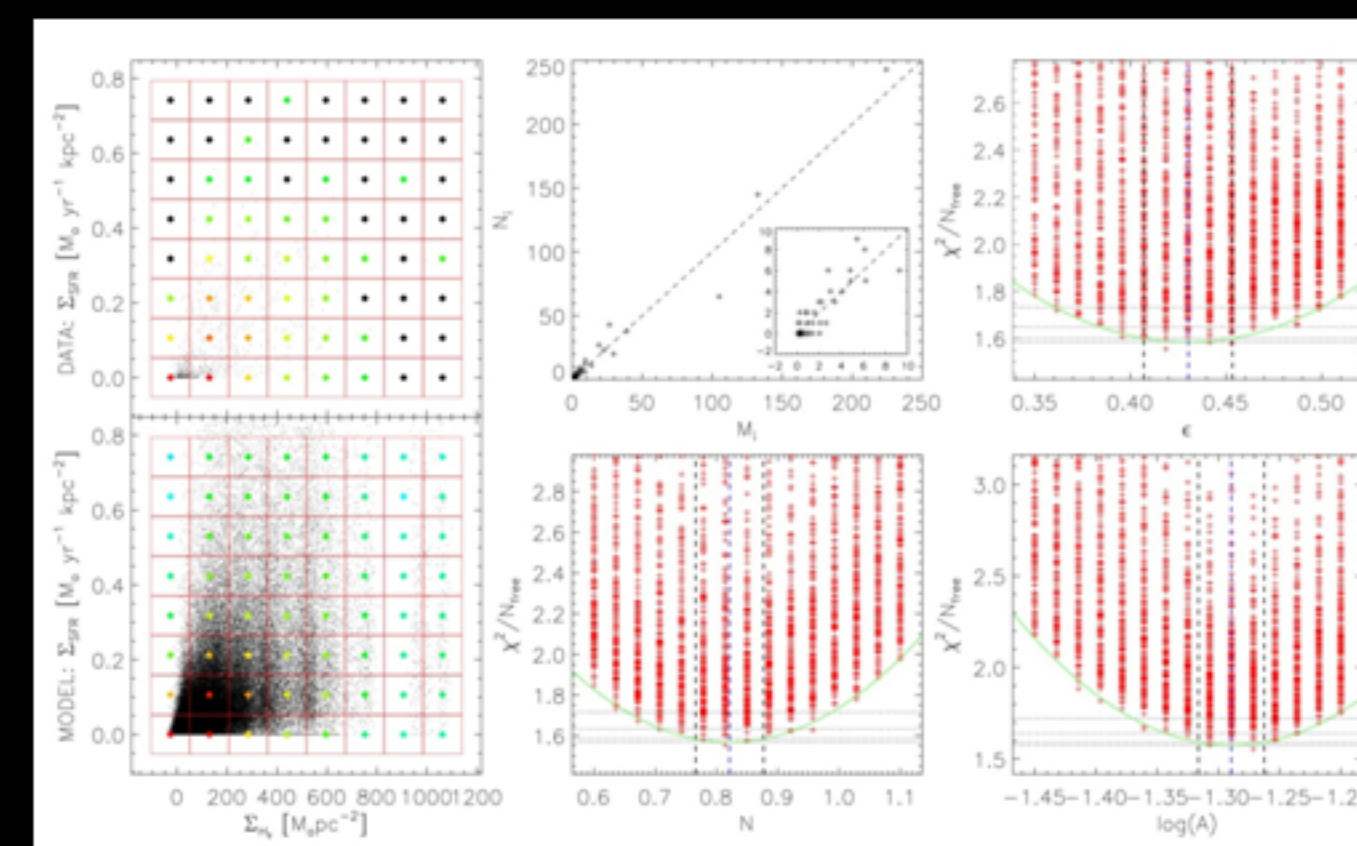
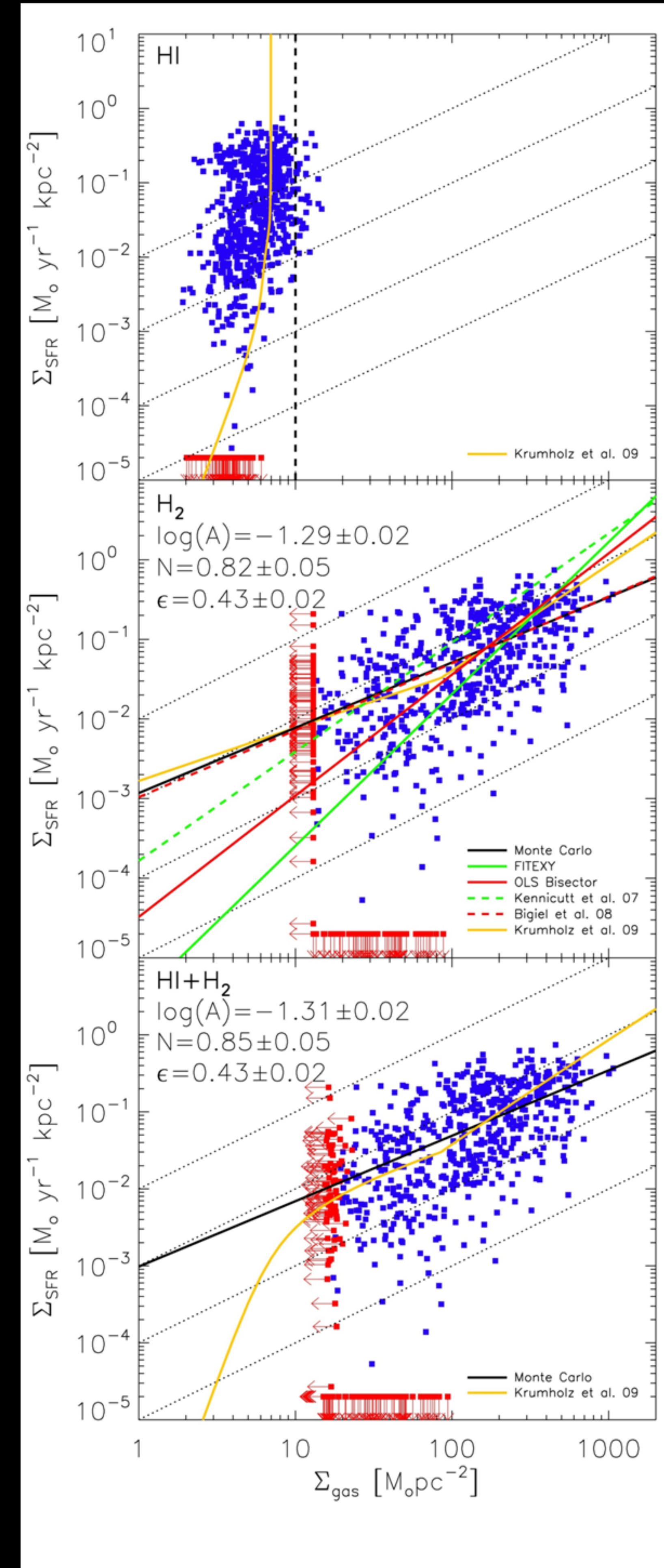


Figure 6: Observed and best-fit model molecular SFL in linear space (left). The data-point density in each grid element is used to compare the model and the data (top-center). Also shown is the  $\chi^2$  distribution for each parameter. Best-fit values and  $1\sigma$  uncertainties are marked by the vertical dashed lines.



## RESULTS

The SFR surface density shows a lack of correlation with the atomic gas surface density, which saturates around  $10 \text{ M}_\odot \text{pc}^{-2}$  (top panel in Figure 7), and a clear correlation with the molecular gas surface density (middle panel in Figure 7), in agreement with previous work by Wong & Blitz (2002), Kennicutt et al. (2007), and Bigiel et al. (2008).

Parametrizing the molecular and total gas SFLs as:  $\frac{\Sigma_{\text{SFR}}}{1 \text{ M}_\odot \text{yr}^{-1} \text{kpc}^{-2}} = A \left( \frac{\Sigma_{\text{gas}}}{100 \text{ M}_\odot \text{pc}^{-2}} \right)^N \times 10^{N(0, \epsilon)}$ , for the molecular gas SFL we measure a slope  $N = 0.82 \pm 0.05$ , an amplitude  $A = 10^{-1.29 \pm 0.02}$ , and an intrinsic scatter  $\epsilon = 0.43 \pm 0.02$  dex. In the central part of NCG 5194 we are sampling a density regime in which the ISM is almost fully molecular, hence the total gas SFL closely follows the molecular SFL and shows very similar best-fit parameters: a slope  $N = 0.85 \pm 0.05$ , an amplitude  $A = 10^{-1.31 \pm 0.02}$ , and an intrinsic scatter  $\epsilon = 0.43 \pm 0.02$  dex.

The slopes we measure are in disagreement with the result of Kennicutt et al. (2007), who measures a strongly super-linear slope for the molecular component (most likely because of differences in the fitting method), but in good agreement with the slope measured for the molecular gas SFL in NGC 5194 by Bigiel et al. (2008). (middle panel in Figure 7). Our results are consistent with the scenario proposed by Bigiel et al. (2008) and Leroy et al. (2008) of a nearly constant SFE in GMCs, which is almost independent of the molecular gas surface density.

We find good agreement with the theoretical SFL model of Krumholz et al. (2009). In their model, the total gas SFL has a super-linear slope  $N = 1.33$  in the high density regime, gets shallower at intermediate densities showing a slope of  $N = 0.67$ , and steepens again at lower densities as the molecular to atomic gas fraction rapidly decreases. Our observations sample the transition between the intermediate and high density regimes in the model. The data does not allow us to observe the predicted kink in the SFL, but our measured slope of 0.85 is very close to what we expect to measure in a region where we sample both the sub-linear and super-linear parts of the SFL in the Krumholz et al. model.

We observe very long depletion timescales of  $\sim 2$  Gyr. This is 100 times longer than the typical GMC free-fall time. The good agreement between our observations and the model implies that this very low efficiency can be easily explained by models in which star-formation is self regulated through turbulence induced by internal mechanical feedback in GMCs.

We measure a large intrinsic scatter of 0.43 dex in both the molecular and total gas SFLs. This is indicative of the existence of further parameters that are important in setting the SFR, although part of the scatter might come from the scatter in the H $\alpha$ -SFR calibration.

Figure 7 (left): Atomic, molecular, and total gas SFLs as measured by VIRUS-P. Upper limits in SFR correspond to regions with  $C_{\text{HII}} = 0$ . Upper limits in  $\Sigma_{\text{H}_2}$  and  $\Sigma_{\text{HI}+\text{H}_2}$  correspond to regions with non-detection in CO at the  $1\sigma$  level. The diagonal dotted lines correspond to constant depletion timescales ( $\text{SFE}^{-1}$ ) of 0.1, 1, 10 and 100 Gyr. Also shown are the Krumholz et al (2009) model, the molecular SFL fits of Kennicutt et al. (2007) and Bigiel et al. (2008), and the results of applying their fitting methods to our data.

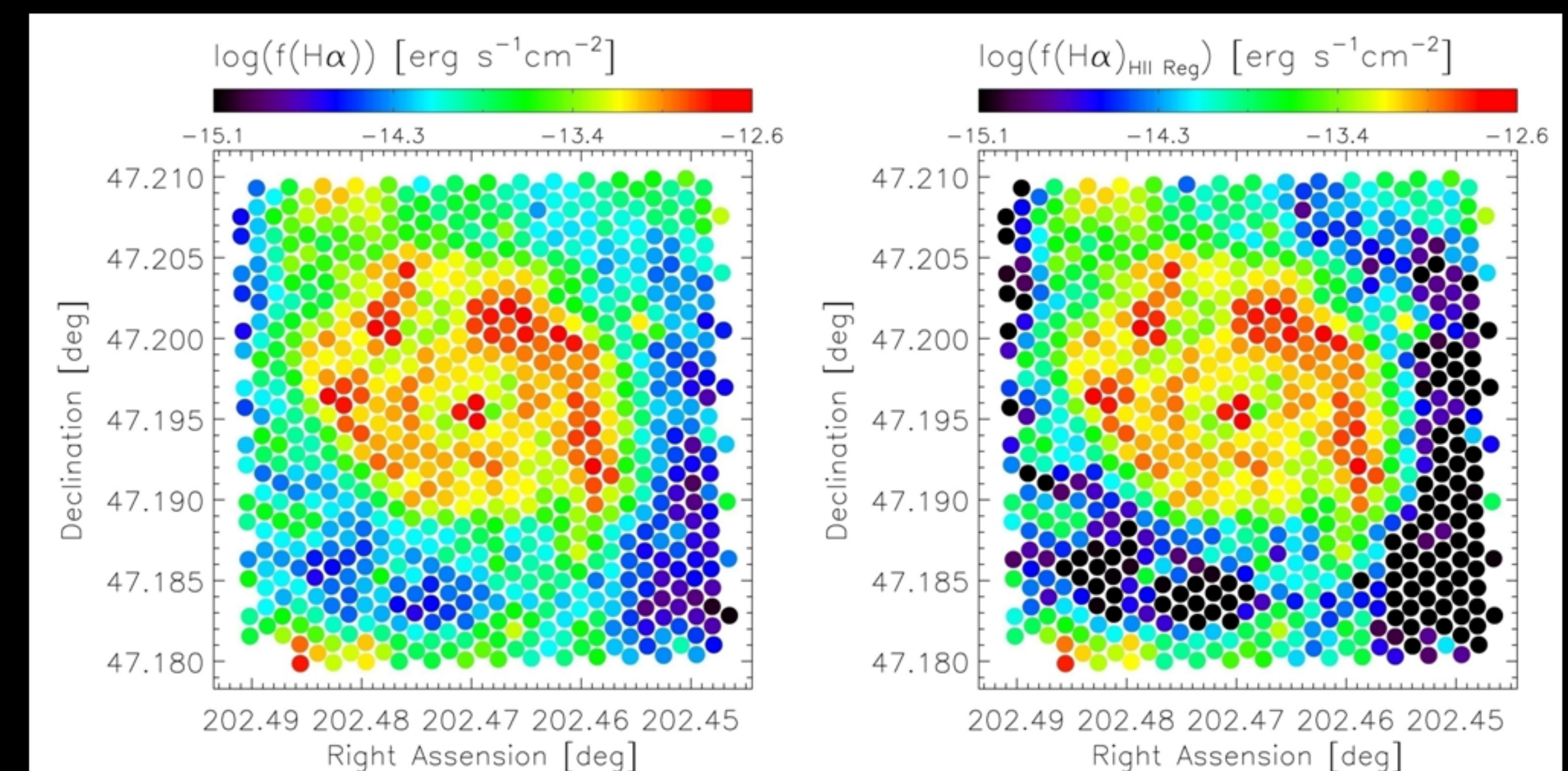


Figure 5: VIRUS-P maps of the extinction corrected H $\alpha$  flux (left), and extinction and DIG corrected H $\alpha$  flux (right) in the central  $4.1 \times 4.1$  kpc<sup>2</sup> of NGC 5194